Analytical model for the composite effect of coupled beams with discrete shear connectors

Tianxin Zheng[1], Yong Lu[*2] and Asif Usmani[2]

[1]*Department of Civil Engineering, University of Nottingham Ningbo, Ningbo, China*
[2]*Institute for Infrastructure and Environment, School of Engineering, The University of Edinburgh,
The King's Buildings, Edinburgh EH9 3JL, UK*

Abstract.   Two-layer coupled or composite beams with discrete shear connectors of finite dimensions are commonly encountered in pre-fabricated construction. This paper presents the development of simplified closed-form solutions for such type of coupled beams for practical applications. A new coupled beam element is proposed to represent the unconnected segments in the beam. General solutions are then developed by an inductive method based on the results from the finite element analysis. A modification is subsequently considered to account for the effect of local deformations. For typical cases where the local deformation is primarily concerned about its distribution over the depth of the coupled beam, empirical modification factors are developed based on parametric calculations using finite element models. The developed analytical method for the coupled beams in question is simple, sufficiently accurate, and suitable for quick calculation in engineering practice.

Keywords: prefabrication; modular structures; coupled beam; discrete shear connection; composite effect; simplified solution

1. Introduction

Pre-fabricated steel structures are increasingly used in modern building construction. In such structures, the occurrence of parallel beams situated one above another with a certain gap in-between are often encountered as a result of assembling pre-fabricated building units. Fig. 1 shows a typical corner-supported module structure (Lawson 2007). Such modular structures are often designed to provide fully open sides and loads are transferred to the corner columns. The modules are transported and assembled onsite, such that adjacent modules are connected by weld or bolts near the top and the bottom of the corner columns, creating a situation with parallel-running beams separated by a sizeable gap.
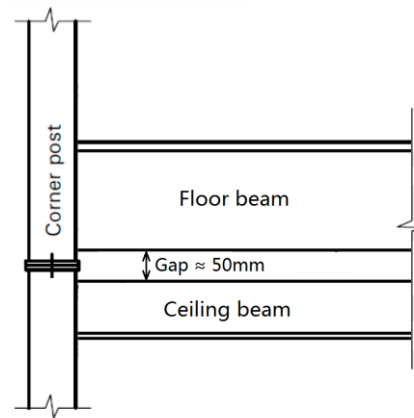
Coupling such two-layer beams to enable effective composite action is obviously beneficial in terms of structural efficiency, saving of structural materials, and increasing the clear internal space of the building. Clearly the best composite performance would be achieved by rigidly bonding the two beams continuously over the entire beam length. However, this is inefficient and labour

---

*Corresponding author, Professor, E-mail: yong.lu@ed.ac.uk

Tianxin Zheng, Yong Lu and Asif Usmani

(a) A typical primary steel frame   (b) Two parallel steel beams separated by a gap

Fig. 1 Corner supported module and connection (after Lawson 2007)

intensive for on-site assembling of the building. It would be more practical to connect the beams in a discrete manner using shear connectors of appropriate dimensions. This produces a special type of two-layer coupled beam with discrete shear connection regions of finite dimensions, both in length and depth.

Conventional composite beams have been widely studied in the last few decades, arguably starting from the well-known Newmark model (Newmark 1951) which was formulated in accordance with the Euler beam theory. The model was then extended to Timoshenko beam with the consideration of the shear effect. The deformable shear connection between laminated layers was firstly considered as continuous, and subsequently discrete shear connections were also involved. Differing from these configurations, however, the present two-layer coupled beam problem involves a sizable gap between the two layers as well as shear connectors of a finite length, which cannot be simply treated as point connections as assumed in some existing two-layer beam models with discrete shear connection (Nguyen *et al*. 2011, Nguyen *et al*. 2010, Nie and Cai 2003). In this respect, the present two-layer coupled beam is called herein as "coupled beam with discrete shear connection regions", or CBDSCR.

In this paper, an analytical method is developed for the evaluation of the composite effect and calculation of the stiffness and deflection in CBDSCR beams. The method is firstly formulated on the basis of simplified plane-section assumptions, leading to a simplified solution for the estimation of the stiffness, as well as the composite effect, of a CBDSCR. The above basic formulation involves only the rigidity (*EI*) of the two beam layers and thus is applicable for both single- and two-material scenarios. The margin and sources of potential errors are subsequently investigated with the aid of refined finite element models. A modification scheme is then introduced to account for the effect of local deformations around the connection regions; and for single-material coupled beams, detailed modification factors are proposed based on numerical parametric calculations using finite element models. The method proposed is simple and yet effective and thus is suitable for quick calculations in practice. Apart from the application in the module building construction, the method can also be applied in cases where stiffer and stronger beams may need to be created by coupling two smaller, standard section beams in an efficient manner.

2. Background theory

Early study of composite beams with flexible shear connection dated back from the well-known Newmark's model (Newmark 1951) for a concrete slab and steel beam composite. Two Euler-Bernoulli beams were used to represent the top slab and the bottom beam, respectively. The model was extended to using Timoshenko beam model, in which the shear deformation of the slab and the beam is taken into account simultaneously (Berczyński and Wróblewski 2005). However, considering the relatively small shear deformation of the concrete slab, a hybrid model (Ranzi and Zona 2007) was subsequently proposed such that the steel beam is represented by Timoshenko beam while Euler-Bernoulli beam is employed for the concrete slab.

The "slip", or in general the relative axial (longitudinal) displacement between the top and bottom beams due to the deformation of the shear connection plays an important role in determining the composite stiffness. The shear connection in Newmark's model allows longitudinal deformation but prevents vertical separation between the beams. In the hybrid model used by Ranzi and Zona (2007), the relative slip is derived from a displacement field considering the axial displacement, rotation and shear deformation. The principle of virtual work is utilized to obtain the weak form of the balance conditions. The integral-type linear viscous-elastic constitutive model is used in the concrete slab, while the steel beam, reinforced bars and shear connectors are considered as linear elastic. The problem is then solved numerically by the finite element method due to the complexity of the governing system of differential equations. Such a solution approach is however difficult to apply for a quick estimation of the stiffness of the composite beam in a design analysis situation. Ranzi *et al.* (2006) extended the displacement field formulation slightly to involve the separation, i.e., relative transverse displacement between the beams. A bi-linear constitutive law was used to simulate the contact behaviour between the beams, with a large normal stiffness being used for penetration penalty.

It is noted that the shear connection in the above laminated beam models is continuous, which may be applicable to welding or gluing (by ideal adhesive) throughout the length, or when the spacing between connectors, such as shear studs, nails, rivets, etc, is small. For composite beams with large spacing (sparse) connectors, a discrete connection model is necessary. Nguyen *et al.* (2011) simulated the sparse shear connector by concentrated spring elements along the axial direction, while transverse separation is prevented. The spring element is a 4-degree of freedom (DOF) element. The unconnected beam segments are modelled by a 10-DOF element, which allows interaction between the two layers, such that the normal force and friction can be taken into account. The plane cross-section assumption is applied on both layers, which however need not be normal to the neutral axis of the composite. The results show that the discrete connection model is more accurate comparing to continuous model if sparse connection is involved.

A number of other studies have also been conducted in the past dealing with extended properties of composite beams, including time-dependant properties of the concrete slab in a discrete connection model (Nguyen *et al.* 2010, Al-deen *et al.* 2011), stiffness reduction due to cracking concrete slab in the hogging moment region (Nguyen *et al.* 2009), vertical uplifting from intermediate supports (Ranzi *et al.* 2010), multi-layered beams (Gianluca 2008), geometric and material nonlinearities (Liang *et al.* 2004), and refined connector behaviour between the beams (Liang *et al.* 2004, Razaqpur and Nofal 1989, Salari *et al.* 1998, Wright 1990).

In spite of the availability of a variety of composite beam models, the essential features of the present CBDSCR beams cannot be properly represented using the existing models. The discrete shear connection regions with sizable dimensions both in the depth (gap) and the length can not be
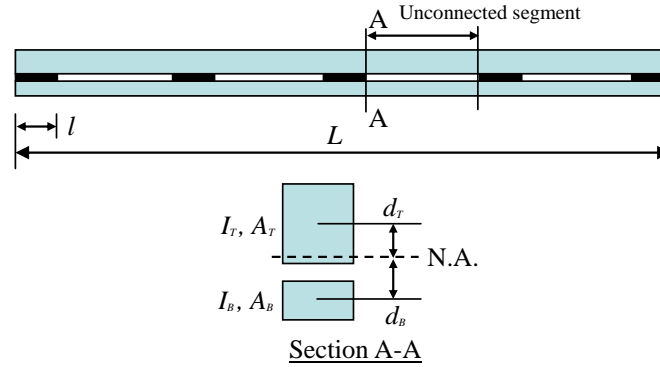
Fig. 2 A typical CBDSCR

simplified either as continuous shear connection or discrete connection with point connectors as studied before. The formulation of sophisticated FE models, as presented in some previous publications (Berczyński and Wróblewski 2005, Ranzi and Zona 2007), is not easy to implement for a practical design analysis. Therefore development of a sufficiently accurate but also easy-to-apply solution for the analysis of CBDSCR becomes necessary.

3. Basic formulation of CBDSCR

3.1 Basic assumptions

The main features of a CBDSCR beam are schematically shown in Fig. 2. The gap between the two layers of the beam may vary, and the connection region is not continuous. Furthermore, the shear connectors can be of significant length. Consequently, the effect of the dimensions of the connection regions, as well as their stiffness, should be appropriately considered in the analysis of the beam.

Three basic assumptions are made firstly in order to develop a basic theoretical model:

(1) No relative slip and separation occurs within the connection regions – this assumption will be compensated by an empirical correction factor to account for the influences of the shear deformation in the connectors as well as local deformation in the vicinity of these regions, which will be presented in the next section;

(2) The top and bottom beams and the connection regions can be described by three Euler beams, respectively;

(3) The top and bottom beams and the connection regions have the same rotation and deflection at their junctions. The cross-section of the junction between a connection region and an unconnected beam segment remains plane during bending. Thus, the compatibility relationship, as shown in Fig. 3, may be written as

$$v_T = v_B = v_C \tag{1a}$$

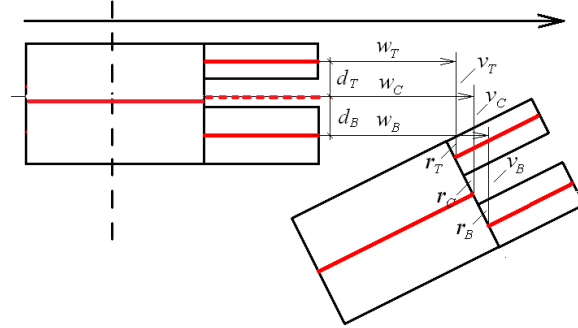$$r_T = r_B = r_C \tag{1b}$$

$$w_T = w_C - r_C d_T \tag{1c}$$

Fig. 3 Compatibility relations at the junction

$$w_B = w_C + r_C d_B \tag{1d}$$

where w is the axial displacement of the neutral axial of the beam, v is the transverse deflection, d is the distance between the neutral axis of the composite section to that of the top/bottom beam, and subscript T, C, B denotes the top, connection and bottom beam, respectively.

As shown in Fig. 2, the reference axis for the coupled beam element is at the neutral axis of the unconnected segment and this is also used for the connected region. It should be noted that in reality the neutral axes of the connected and unconnected regions are not actually co-linear. This may cause a difference in the axial deformation between the connected and unconnected regions at the junction, but since the rotation and deflection have been assumed to maintain the same at the junction, the derived flexural stiffness (rigidity) of the coupled beam would not be affected significantly by the simplification in the reference axis. The influence becomes further negligible by the fact that the depth of the shear connectors is usually much smaller than the depths of the top and bottom beams in practice, therefore the two neutral axes are effectively quite close to each other.

3.2 Stiffness matrix of unconnected beam segments

According to the compatibility relations described in Eq. (1), the unconnected two-layer beam segments (see Fig. 2(b)) can be simplified into a coupled element whose stiffness can be derived from the basic beam element formulation, as follows.

The general constitutive equation of the original two-beam segments may be written as

$$\mathbf{K}\boldsymbol{\delta} = \mathbf{F} \tag{2}$$

in which the displacement vector has 12 elements, including 3 DOFs (transverse displacement, axial displacement and rotation) at each of the four ends of the top and bottom beam

$$\boldsymbol{\delta} = \left\{ w_{T1} \quad v_{T1} \quad r_{T1} \quad w_{T2} \quad v_{T2} \quad r_{T2} \quad w_{B1} \quad v_{B1} \quad r_{B1} \quad w_{B2} \quad v_{B2} \quad r_{B2} \right\}^T \tag{3}$$

The stiffness matrix of the coupled element is represented by the assembly of the element stiffness matrix of the two beams

$$\mathbf{K} = \begin{bmatrix} \mathbf{K_T} & \mathbf{0} \\ \mathbf{0} & \mathbf{K_B} \end{bmatrix} \tag{4}$$

$$\mathbf{K_e} = \begin{bmatrix} \dfrac{E_e A_e}{L_e} & 0 & 0 & -\dfrac{E_e A_e}{L_e} & 0 & 0 \\ 0 & \dfrac{12E_e I_e}{L_e^3} & \dfrac{6E_e I_e}{L_e^2} & 0 & -\dfrac{12E_e I_e}{L_e^3} & \dfrac{6E_e I_e}{L_e^2} \\ 0 & \dfrac{6E_e I_e}{L_e^2} & \dfrac{4E_e I_e}{L_e} & 0 & -\dfrac{6E_e I_e}{L_e^2} & \dfrac{2E_e I_e}{L_e} \\ -\dfrac{E_e A_e}{L_e} & 0 & 0 & \dfrac{E_e A_e}{L_e} & 0 & 0 \\ 0 & -\dfrac{12E_e I_e}{L_e^3} & -\dfrac{6E_e I_e}{L_e^2} & 0 & \dfrac{12E_e I_e}{L_e^3} & -\dfrac{6E_e I_e}{L_e^2} \\ 0 & \dfrac{6E_e I_e}{L_e^2} & \dfrac{2E_e I_e}{L_e} & 0 & -\dfrac{6E_e I_e}{L_e^2} & \dfrac{4E_e I_e}{L_e} \end{bmatrix} \tag{5}$$

The subscript e stands for T or B for the top and bottom beam, respectively. The constraint equations from the compatibility relationship in Eq. (1) are expressed by

$$w_{T1} = w_{C1} - d_T r_{C1} \tag{6a}$$

$$v_{T1} = v_{C1} \tag{6b}$$

$$r_{T1} = r_{C1} \tag{6c}$$

$$w_{T2} = w_{C2} - d_T r_{C2} \tag{6d}$$

$$v_{T2} = v_{C2} \tag{6e}$$

$$r_{T2} = r_{C2} \tag{6f}$$

$$w_{B1} = w_{C1} + d_B r_{C1} \tag{6g}$$

$$v_{B1} = v_{C1} \tag{6h}$$

$$r_{B1} = r_{C1} \tag{6i}$$

$$w_{B2} = w_{C2} + d_B r_{C2} \tag{6j}$$

$$v_{B2} = v_{C2} \tag{6k}$$

$$r_{B2} = r_{C2} \tag{6l}$$

With these coupling equations, the 12-DOF displacement vector reduces to a 6-DOF vector, as illustrated in Fig. 4

$$\boldsymbol{\delta}^* = \{ w_{C1} \quad v_{C1} \quad r_{C1} \quad w_{C2} \quad v_{C2} \quad r_{C2} \}^T \tag{7}$$

The corresponding constitutive relations for the 6-DOF element is

$$\mathbf{K}^* \boldsymbol{\delta}^* = \mathbf{F}^* \tag{8a}$$

$$\boldsymbol{\delta} = \mathbf{T_c} \boldsymbol{\delta}^* \tag{8b}$$
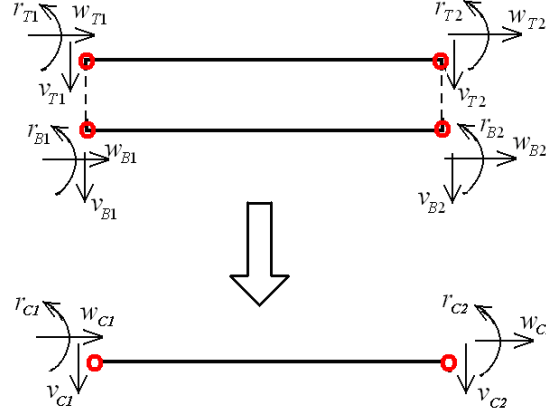
$$\mathbf{F}^* = \mathbf{T_c}^T \mathbf{F} \tag{8c}$$

Fig. 4 A new combined element for a two-layer unconnected beam segment

$$\mathbf{K}^* = \mathbf{T_c}^T \mathbf{K} \mathbf{T_c} \tag{8d}$$

in which $\mathbf{T_c}$ is the transform matrix determined by the coupling equations

$$\mathbf{T_c} = \begin{bmatrix}
1 & 0 & -d_T & 0 & 0 & 0 \\
0 & 1 & 0 & 0 & 0 & 0 \\
0 & 0 & 1 & 0 & 0 & 0 \\
0 & 0 & 0 & 1 & 0 & -d_T \\
0 & 0 & 0 & 0 & 1 & 0 \\
0 & 0 & 0 & 0 & 0 & 1 \\
1 & 0 & d_B & 0 & 0 & 0 \\
0 & 1 & 0 & 0 & 0 & 0 \\
0 & 0 & 1 & 0 & 0 & 0 \\
0 & 0 & 0 & 1 & 0 & d_B \\
0 & 0 & 0 & 0 & 1 & 0 \\
0 & 0 & 0 & 0 & 0 & 1
\end{bmatrix} \tag{9}$$

For generality the Young's modulus of the top and bottom beams is assumed to be E_T and E_B, respectively, thus allowing for applications where different materials are used. Subsequently, the stiffness matrix of the combined element is reduced to a 6-DOF stiffness matrix as

$$\mathbf{K}^* = \begin{bmatrix}
\frac{E_T A_T + E_B A_B}{L} & 0 & \frac{E_B A_B d_B - E_T A_T d_T}{L} & -\frac{E_T A_T + E_B A_B}{L} & 0 & \frac{E_T A_T d_T - E_B A_B d_B}{L} \\
0 & \frac{12(E_T I_T + E_B I_B)}{L^3} & \frac{6(E_T I_T + E_B I_B)}{L^2} & 0 & -\frac{12(E_T I_T + E_B I_B)}{L^3} & \frac{6(E_T I_T + E_B I_B)}{L^2} \\
\frac{E_B A_B d_B - E_T A_T d_T}{L} & \frac{6(E_T I_T + E_B I_B)}{L^2} & \frac{E_T A_T d_T{}^2 + E_B A_B d_B{}^2 + 4(E_T I_T + E_B I_B)}{L} & \frac{E_T A_T d_T - E_B A_B d_B}{L} & -\frac{6(E_T I_T + E_B I_B)}{L^2} & \frac{-E_T A_T d_T{}^2 - E_B A_B d_B{}^2 2(E_T I_T + E_B I_B)}{L} \\
-\frac{E_T A_T + E_B A_B}{L} & 0 & \frac{E_T A_T d_T - E_B A_B d_B}{L} & \frac{E_T A_T + E_B A_B}{L} & 0 & \frac{E_B A_B d_B - E_T A_T d_T}{L} \\
0 & -\frac{12(E_T I_T + E_B I_B)}{L^3} & -\frac{6(E_T I_T + E_B I_B)}{L^2} & 0 & \frac{12(E_T I_T + E_B I_B)}{L^3} & -\frac{6(E_T I_T + E_B I_B)}{L^2} \\
\frac{E_T A_T d_T - E_B A_B d_B}{L} & \frac{6(E_T I_T + E_B I_B)}{L^2} & \frac{-E_T A_T d_T{}^2 - E_B A_B d_B{}^2 + 2(E_T I_T + E_B I_B)}{L} & \frac{E_B A_B d_B - E_T A_T d_T}{L} & -\frac{6(E_T I_T + E_B I_B)}{L^2} & \frac{E_T A_T d_T{}^2 + E_B A_B d_B{}^2 + 4(E_T I_T + E_B I_B)}{L}
\end{bmatrix} \tag{10}$$

Since d_T and d_B is the distance between the neutral axis of the top and bottom beam, respectively, to the neutral axis of the composite section, it has the following relation

$$E_B A_B d_B = E_T A_T d_T \tag{11}$$

Therefore, $\mathbf{K}^*$ in Eq. (10) is simplified into

$$\mathbf{K}^* = \begin{bmatrix}
\frac{E_T A_T + E_B A_B}{L} & 0 & 0 & -\frac{E_T A_T + E_B A_B}{L} & 0 & 0 \\
0 & \frac{12(E_T I_T + E_B I_B)}{L^3} & \frac{6(E_T I_T + E_B I_B)}{L^2} & 0 & -\frac{12(E_T I_T + E_B I_B)}{L^3} & \frac{6(E_T I_T + E_B I_B)}{L^2} \\
0 & \frac{6(E_T I_T + E_B I_B)}{L^2} & \frac{E_T A_T d_T{}^2 + E_B A_B d_B{}^2 + 4(E_T I_T + E_B I_B)}{L} & 0 & -\frac{6(E_T I_T + E_B I_B)}{L^2} & \frac{-E_T A_T d_T{}^2 - E_B A_B d_B{}^2 2(E_T I_T + E_B I_B)}{L} \\
-\frac{E_T A_T + E_B A_B}{L} & 0 & 0 & \frac{E_T A_T + E_B A_B}{L} & 0 & 0 \\
0 & -\frac{12(E_T I_T + E_B I_B)}{L^3} & -\frac{6(E_T I_T + E_B I_B)}{L^2} & 0 & \frac{12(E_T I_T + E_B I_B)}{L^3} & -\frac{6(E_T I_T + E_B I_B)}{L^2} \\
0 & \frac{6(E_T I_T + E_B I_B)}{L^2} & \frac{-E_T A_T d_T{}^2 - E_B A_B d_B{}^2 + 2(E_T I_T + E_B I_B)}{L} & 0 & -\frac{6(E_T I_T + E_B I_B)}{L^2} & \frac{E_T A_T d_T{}^2 + E_B A_B d_B{}^2 + 4(E_T I_T + E_B I_B)}{L}
\end{bmatrix} \tag{12a}$$

Elements in $\mathbf{K}^*$ indicate that the coupled beam element can be considered as the summation of the stiffness of the two individual beams plus an additional (composite) stiffness term $\Delta(EI)/L=(E_T A_T d_T{}^2+E_B A_B d_B{}^2)/L$, with ($EI$) denoting an equivalent flexural rigidity. $\mathbf{K}^*$ can be further written as

$$\mathbf{K}^* = \mathbf{K_T} + \mathbf{K_B} + \begin{bmatrix}
0 & 0 & 0 & 0 & 0 & 0 \\
0 & 0 & 0 & 0 & 0 & 0 \\
0 & 0 & \frac{\Delta(EI)}{L} & 0 & 0 & -\frac{\Delta(EI)}{L} \\
0 & 0 & 0 & 0 & 0 & 0 \\
0 & 0 & 0 & 0 & 0 & 0 \\
0 & 0 & -\frac{\Delta(EI)}{L} & 0 & 0 & \frac{\Delta(EI)}{L}
\end{bmatrix} \tag{12b}$$

Any distributed load applied over an unconnected segment is converted to point loads applied at the ends of the coupled beam element, as per the standard procedure for a conventional beam element.

3.3 Solution of deflection using the coupled beam element

With the above formulated coupled beam element for the unconnected beam segments, a CBDSCR beam can be modelled as a combination of the coupled elements (for unconnected segments) and the conventional beam elements (for the connection regions). Subsequently, it is possible to derive a closed-form solution for a CBDSCR beam under a standard loading condition. Details of the solutions will be given later in the Section 4. An example is shown in what follows.

Consider a simply-supported CBDSCR with 5 evenly distributed connection regions dividing the beam into 4 segments (refer to Fig. 2). The length of each unconnected segment is thus $(L-5l)/4$, with L being the total length of the beam and l the length of a connection region. It is noted that the depth of the shear connectors is usually much smaller than the depths of the top and bottom beams, therefore the flexible rigidity of cross-section in the connection region may be approximated as $E_T A_T d_T{}^2+E_B A_B d_B{}^2+E_T I_T+E_B I_B$. After assembling the stiffness matrix of the overall beam with 5 conventional beam elements for the connection regions and 4 coupled beam elements

for the unconnected beam segments, an analytical solution can be obtained. The solution for the maximum deflection when the beam is subjected to a mid-span point load F is as follows

$$\delta_{\max} = \frac{FL^3\left[16\left(E_T I_T + E_B I_B\right)+\left(1-\frac{5l}{L}\right)^3\left(E_T A_T d_T{}^2 + E_B A_B d_b^2\right)\right]}{768\left(E_T I_T + E_B I_B\right)\left(E_T I_T + E_B I_B + E_T A_T d_T{}^2 + E_B A_B d_b^2\right)} \tag{13a}$$

If the length of the connection region of the CBDSCR is negligible, the solution reduces to:

$$\delta_{\max} = \frac{FL^3\left[16\left(E_T I_T + E_B I_B\right)+\left(E_T A_T d_T^2 + E_B A_B d_b^2\right)\right]}{768\left(E_T I_T + E_B I_B\right)\left(E_T I_T + E_B I_B + E_T A_T d_T^2 + E_B A_B d_b^2\right)} \tag{13b}$$

4. Generalised stiffness of CBDSCR and parametric analysis

4.1 Equivalent sectional rigidity and derivation

The stiffness of a CBDSCR with a specific boundary condition, force and connection region configurations can be obtained theoretically using a similar procedure as described earlier in Section 3.2. Consider the solution in Eq. (13), the maximum deflection $\delta_{\max}$ of an equivalent uniform beam with an equivalent flexural rigidity $(EI)_{eq}$ subjected to a mid-span concentrated force is calculated as

$$\delta_{\max} = \frac{FL^3}{48(EI)_{eq}} \tag{14}$$

Substitute Eq. (13b), $(EI)_{eq}$ is obtained as

$$(EI)_{eq} = \frac{1}{\dfrac{1}{16}\cdot\dfrac{E_T A_T d_T{}^2 + E_B A_B d_B{}^2}{E_T I_T + E_B I_B}+1}\left(E_T I_T + E_B I_B + E_T A_T d_T{}^2 + E_B A_B d_B{}^2\right) \tag{15a}$$

Let

$$(EI)_O = E_T I_T + E_B I_B \tag{15b}$$

$$(EI)_C = E_T I_T + E_B I_B + E_T A_T d_T{}^2 + E_B A_B d_B{}^2 \tag{15c}$$

$$\Delta(EI) = EI_C - EI_O = E_T A_T d_T{}^2 + E_B A_B d_B{}^2 \tag{15d}$$

where $(EI)_O$ is the summation of the flexural rigidity of the top and the bottom beams, $(EI)_C$ is the bending rigidity of the ideal composite beam, $\Delta(EI)$ is the increase of the flexural rigidity of section due to the ideal composite effect. Thus

$$(EI)_{eq} = \frac{1}{\dfrac{1}{16}\dfrac{\Delta(EI)}{(EI)_O}+1}(EI)_C \tag{15e}$$

Eq. (15e) may be written in a general form as

$$(EI)_{eq} = \frac{1}{\beta \dfrac{\Delta(EI)}{(EI)_O} + 1}(EI)_C = \alpha(EI)_C \tag{15f}$$

$$\alpha = \frac{1}{\beta \dfrac{\Delta(EI)}{(EI)_O} + 1} \tag{15g}$$

where α is the coefficient of the composite effect of the CBDSCR, β is a factor related to the boundary condition, loading condition and number of the segments of a CBDSCR.

For the example CBDSCR with 4 evenly divided segments and a negligible connection region length, $\beta = 1/16$. Conducting a similar analysis on CBDSCRs with different boundary and loading conditions and number of segments, $(EI)_{eq}$ for a variety of CBDSCRs can be determined and the results in terms of the coefficient β are shown in Table 1. It can be observed that the factor β can be expressed as a function of the number of the unconnected beam segments, n, as follows:

a) For simply- supported (**SS**) beams under a mid-span concentrated load (**CL**)

$$\beta = \begin{cases} \dfrac{1}{n^2} & n = \text{even number} \\[2ex] \dfrac{4n-3}{4n^3} & n = \text{odd number} \end{cases} \tag{16a}$$

b) For simply-supported beams under a uniformly distributed load (**UDL**)

$$\beta = \begin{cases} \dfrac{4}{5n^2} & n = \text{even number} \\[2ex] \dfrac{4n^2-3}{5n^4} & n = \text{odd number} \end{cases} \tag{16b}$$

c) For fixed-support (**FS**) beams under a mid-span concentrated load

$$\beta = \begin{cases} \dfrac{4}{n^2} & n = \text{even number} \\[2ex] \dfrac{4n-3}{n^3} & n = \text{odd number} \end{cases} \tag{16c}$$

d) For fixed-support beams under a uniformly distributed load

$$\beta = \begin{cases} \dfrac{4}{n^2} & n = \text{even number} \\[2ex] \dfrac{4n^2-3}{n^4} & n = \text{odd number} \end{cases} \tag{16d}$$

Table 1 β values for a CBDSCR with n evenly distributed unconnected segments, assuming a negligible connection region length

Number of unconnected segments n	β values in $(EI)_{eq}$			
	SS and CL	**FS and CL**	**SS and UDL**	**FS and UDL**
2	$\dfrac{1}{4}$	1	$\dfrac{1}{5}$	1
3	$\dfrac{1}{12}$	$\dfrac{1}{3}$	$\dfrac{11}{135}$	$\dfrac{11}{27}$
4	$\dfrac{1}{16}$	$\dfrac{1}{4}$	$\dfrac{1}{20}$	$\dfrac{1}{4}$
5	$\dfrac{17}{500}$	$\dfrac{17}{125}$	$\dfrac{97}{3125}$	$\dfrac{97}{625}$
6	$\dfrac{1}{36}$	$\dfrac{1}{9}$	$\dfrac{1}{45}$	$\dfrac{1}{9}$
7	$\dfrac{25}{1372}$	$\dfrac{25}{343}$	$\dfrac{193}{12005}$	$\dfrac{193}{2401}$
8	$\dfrac{1}{64}$	$\dfrac{1}{16}$	$\dfrac{1}{80}$	$\dfrac{1}{16}$
9	$\dfrac{11}{972}$	$\dfrac{1}{243}$	$\dfrac{321}{32805}$	$\dfrac{321}{6561}$
10	$\dfrac{1}{100}$	$\dfrac{1}{25}$	$\dfrac{1}{125}$	$\dfrac{1}{25}$

SS: simple-support, FS: fixed-support,
CL: concentrated loading at mid-span, UDL: uniformly distributed loading

Eq. (16) indicate that β reduces exponentially with the increase of n. The maximum difference in the β values between the two loading patterns is about 25% in simply supported beams, whereas the difference is less significant in the fixed-support beams. The variation of the composite coefficient α with n is dependent upon β as well as the specific sectional properties. α calculated from Eq. (15g) increases with the increase of n.

If the length of the connection region is considered, $(EI)_{eq}$ in Table 1 is modified as shown in Table 2. Correspondingly, the composite coefficient α may be expressed similarly as Eq. (15g) with the introduction of a factor γ, as

$$\alpha = \frac{1}{\beta\gamma\dfrac{\Delta EI}{EI_O}+1} \tag{17a}$$

where

$$\gamma = \left[1-\frac{(n+1)l}{L}\right]^3 \qquad \text{for concentrated load} \tag{17b}$$

$$\gamma \approx \left[1-\frac{(n+1)l}{L}\right]^3\left(1-\frac{l}{L}\right) \qquad \text{for uniformly distributed load} \tag{17c}$$

Table 2 I_{eq} of a CBDSCR with **n** evenly distributed unconnected segments, assuming non-negligible connection region length[*]

I_{eq}			
SS and CL	**FS and CL**	**SS and UDL**	**FS and UDL**
$\dfrac{I_C}{\dfrac{\Delta I}{4I_O}\left(1-\dfrac{3l}{L}\right)^3+1}$	$\dfrac{I_C}{\dfrac{\Delta I}{I_O}\left(1-\dfrac{3l}{L}\right)^3+1}$	$\dfrac{I_C}{\dfrac{\Delta I}{5I_O}\left(1-\dfrac{3l}{L}\right)^3\left(1-\dfrac{l}{L}\right)+1}$	$\dfrac{I_C}{\dfrac{\Delta I}{I_O}\left(1-\dfrac{3l}{L}\right)^3\left(1-\dfrac{l}{L}\right)+1}$
$\dfrac{I_C}{\dfrac{\Delta I}{12I_O}\left(1-\dfrac{4l}{L}\right)^3+1}$	$\dfrac{I_C}{\dfrac{\Delta I}{3I_O}\left(1-\dfrac{4l}{L}\right)^3+1}$	$\dfrac{I_C}{\dfrac{11\Delta I}{1351I_O}\left(1-\dfrac{4l}{L}\right)^3\left(1-\dfrac{12l}{11L}\right)+1}$	$\dfrac{I_C}{\dfrac{11\Delta I}{27I_O}\left(1-\dfrac{4l}{L}\right)^3\left(1-\dfrac{12l}{L}\right)+1}$
$\dfrac{I_C}{\dfrac{\Delta I}{16I_O}\left(1-\dfrac{5l}{L}\right)^3+1}$	$\dfrac{I_C}{\dfrac{\Delta I}{4I_O}\left(1-\dfrac{5l}{L}\right)^3+1}$	$\dfrac{I_C}{\dfrac{\Delta I}{20I_O}\left(1-\dfrac{5l}{L}\right)^3\left(1-\dfrac{l}{L}\right)+1}$	$\dfrac{I_C}{\dfrac{\Delta I}{4I_O}\left(1-\dfrac{5l}{L}\right)^3\left(1-\dfrac{l}{L}\right)+1}$
$\dfrac{I_C}{\dfrac{17\Delta I}{500I_O}\left(1-\dfrac{6l}{L}\right)^3+1}$	$\dfrac{I_C}{\dfrac{17\Delta I}{500I_O}\left(1-\dfrac{6l}{L}\right)^3+1}$	$\dfrac{I_C}{\dfrac{97\Delta I}{31251I_O}\left(1-\dfrac{6l}{L}\right)^3\left(1-\dfrac{102l}{97L}\right)+1}$	$\dfrac{I_C}{\dfrac{97\Delta I}{625I_O}\left(1-\dfrac{6l}{L}\right)^3\left(1-\dfrac{102l}{97L}\right)+1}$

*Note: For coupled beam with two different materials, all "I" terms in the table are changed to "(EI)", e.g., I_{eq} to EI_{eq}, I_C to $(EI)_C$, and the same formulas apply.

Table 3 List of CBDSCRs used in comparison

Beam	l (mm)	h_T (mm)	g (mm)	n	Bonding conditions	Loading
1	200	100	20	4	SS	CL: 1000N at mid span
2	200	100	20	4	SS	UDL: 1000N/m
3	200	100	20	4	FS	CL: 1000N at mid span
4	200	100	20	4	FS	UDL: 1000N/m
5	200	100	20	5	SS	CL: 1000N at mid span
6	200	100	20	6	SS	CL: 1000N at mid span
7	200	100	30	4	SS	CL: 1000N at mid span
8	200	100	50	4	SS	CL: 1000N at mid span
9	400	100	20	4	SS	CL: 1000N at mid span
10	600	100	20	4	SS	CL: 1000N at mid span
11	200	150	20	4	SS	CL: 1000N at mid span
12	200	200	20	4	SS	CL: 1000N at mid span

4.2 Verification with refined finite element model

In order to verify the accuracy of the theoretical solution, a number of CBDSCR beams are constructed and calculated using both the theoretical solution and refined finite element models. The beams are assumed to be made of steel with a Young's modulus of 210 GPa and a Poisson's ratio of 0.3, and have the same overall length of 5.0m. The top and bottom beams are of rectangular cross-section with a uniform width of 0.1m, and the depth of the bottom beam is fixed at 100mm. Totally 12 CBDSCR beam scenarios are constructed for comparison, with variations in the loading patterns, boundary conditions, number of unconnected segments, height of the gap,

Table 4 Comparison of maximum deflections predicted using the proposed beam model with FE results

Beam	FE model δ_{max} (mm)	Eq. (15) (without connection length)			Eq. (17) (with connection length)		
		α	δ_{max} (mm)	Error	α	δ_{max} (mm)	Error
1	0.164	0.79	0.178	8.1%	0.88	0.159	-3.1%
2	0.495	0.82	0.531	7.2%	0.90	0.483	-2.5%
3	0.059	0.48	0.073	22.9%	0.64	0.054	-8.3%
4	0.015	0.48	0.018	25.3%	0.65	0.013	-7.8%
5	0.152	0.85	0.164	7.7%	0.93	0.150	-1.2%
6	0.149	0.89	0.157	4.9%	0.96	0.146	-2.2%
7	0.148	0.76	0.161	8.9%	0.86	0.142	-3.9%
8	0.123	0.70	0.136	10.3%	0.82	0.116	-5.8%
9	0.151	0.79	0.178	17.4%	0.94	0.148	-2.1%
10	0.144	0.79	0.178	23.2%	0.98	0.142	-1.4%
11	0.088	0.82	0.092	4.6%	0.90	0.084	-4.6%
12	0.052	0.86	0.053	1.2%	0.92	0.049	-5.8%

length of the connection region, and the height of the top beam, as summarised in Table 3. A refined finite element model is employed to model the CBDSCRs. Element PLANE42 in ANSYS is used to construct the FE model. The mesh of the FE model is made sufficiently fine such that at least 6 plane elements are used over the height of each component beam, which proved to be adequate after a mesh convergence check.

Table 4 compares the mid-span deflections of the 12 CBDSCRs calculated by Eqs. (15) and (17) and the results obtained using the refined plane element models. As the length of each connection region in all the cases is substantial comparing to the total depth of the composite beam, ignoring the connection length (i.e., assuming point connections and using Eq. (15)) results in larger errors, and in some cases the error is up to about 26%. On the other hand, with the consideration of the connection length, i.e., using Eq. (17), the theoretical predictions match the FE results satisfactorily and the maximum error is less than 9%.

4.3 Factors influencing the composite effect of CBDSCR

It can be generally understood that the composite effect in a CBDSCR is affected by the following main factors, i) the differential bending stiffness between that of the full composite section and that of the uncoupled section, which effectively defines the overall demand on the connectors and is closely associated with the gap size between the top and bottom parts of the beam, ii) spacing or the number of the shear connectors, iii) the length of each connector, and iv) the shear stiffness of the connectors themselves. Herein we assume a sufficiently large stiffness in the connectors. The influences of the remaining factors can be evaluated based on the theoretical solution given in Eqs. (15) and (17). For simplicity, we shall first examine the situation where the top and bottom parts of the CBDSCR have identical section properties.

a) The differential flexural rigidity $\Delta(EI)/(EI)_O$
From Eqs. (15) and (17) it can be understood that the stiffness of a CBDSCR, and hence the composite coefficient, will decrease with the increase of the differential bending rigidity $\Delta(EI)/(EI)_O$. For the case of beam-1 described in Section 4.2, when the gap depth g increases from
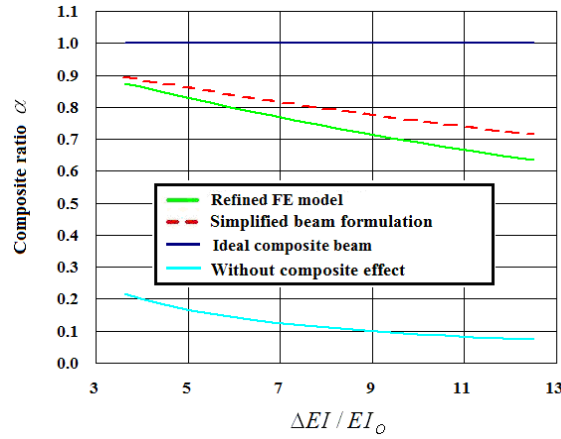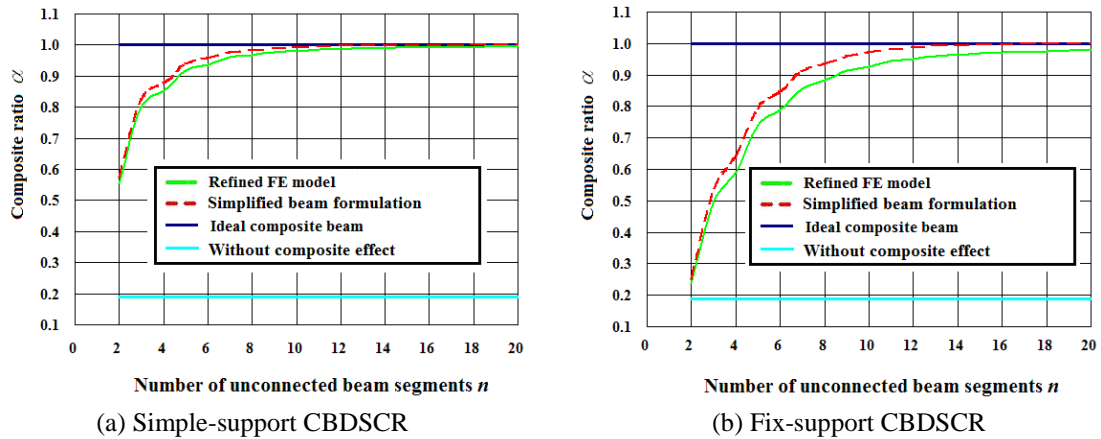
Fig. 5 Effect of $\Delta(EI)/(EI)_O$ on α

(a) Simple-support CBDSCR (b) Fix-support CBDSCR

Fig. 6 Effect of number of shear connectors

0.01 m to 0.10 m, $\Delta(EI)/(EI)_O$ increases from 3.6 to 12.5. Fig. 5 shows a persistent decrease of the theoretical α; the FEA results agree reasonably well with the theoretical solution with slightly increasing discrepancy as $\Delta(EI)/(EI)_O$ increases. The discrepancy will be discussed in the next section.

b) Number of unconnected segments n

Increasing the number of the shear connectors results in an increase of the number of unconnected segments, denoted by n, and is expected to enhance the overall composite effect, and hence increasing the composite ratio α of a CBDSCR. Fig. 6 shows the variation of α with n in both simply-support and fixed-support conditions. The theoretical curves agree reasonably well with the FEA results. α increases and eventually approaches 1.0 with the increase of n. In the simple-support cases, α increases from 0.58 in the 2-segment case to 0.82 in the 3-segment and 0.94 in the 5-segment cases. In the fixed-support cases, where the two end supports serve as connectors themselves, α increase from 0.25 in 2-segment case to 0.80 in the 5-connector case and 0.91 in the 7-segments case.

(a) *n*=4   (b) *n*=6
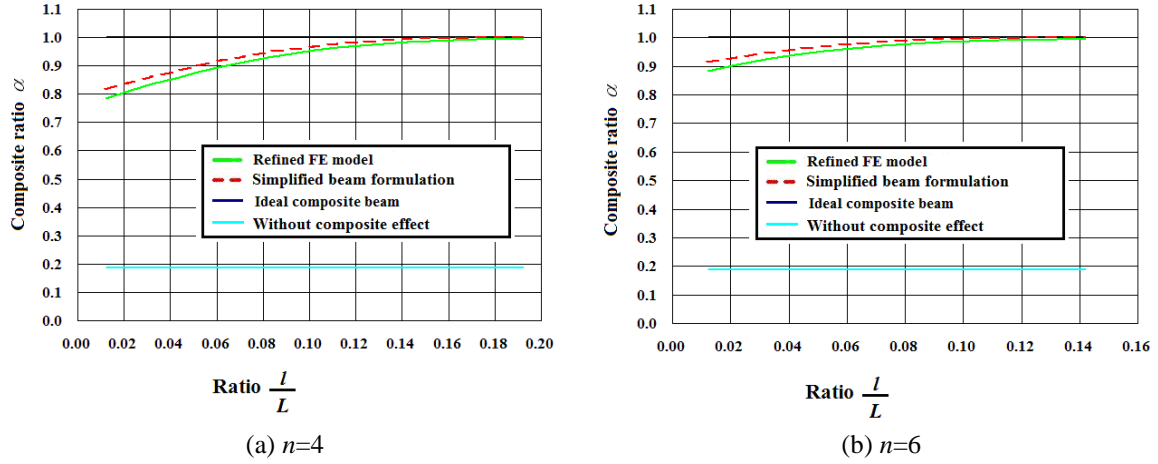
Fig. 7 Effect of length ratio *l/L* of the connection region

c) Relative length of the shear connection region

Similar to increasing the number of connectors, a larger connector length (*l*) is expected to lead to a better coupling effect between the top and bottom beams. Eq. (17) shows that increasing *l* reduces γ, and as a result α increases. Fig. 7 shows the influencing trend of *l/L* on the composite effect in a simply supported CBSDCR with the number of shear connectors (*n*) being 4 and 6, respectively. It can observed that for the case *n*=4, with *l/L* increasing from 0.01 to 0.19, α increases from 0.82 to 1.0; for the case *n*=6, with *l/L* increasing from 0.01 to 0.14, α increases from 0.92 to 1.0.

5. Modification to basic formulation considering local deformation

5.1 Local deformation and stress distribution around connection regions

The basic formulation for CBDSCR presented above has assumed that the cross-section at the junction between the connectors and the unconnected segments remain plane during bending. This assumption is apparently a source of errors in the predicted beam responses. To illustrate this, we create a modified FE model in which rigid beam elements are inserted vertically at all junction sections, as shown in Fig. 8(a), such that these sections are artificially constrained to deform as plane sections. Fig. 8(b) shows a comparison of the resulting composite ratio α between the two FE models as well as that predicted using the basic beam formulation. It can be observed that the results from the modified FE model match closely the simplified beam formulation, and both results exhibit similar overestimation of the composite effect as compared with the original FE model. This indicates that the plane cross-section assumption at the junctions is indeed the major source of the discrepancy in the predicted beam response with the proposed beam formulation.

Rigid beams on the two sides connection region

(a) FE model with artificial plane section (rigid elements) inserted at the junction interfaces

(b) Variation of composite effect predicted using different models
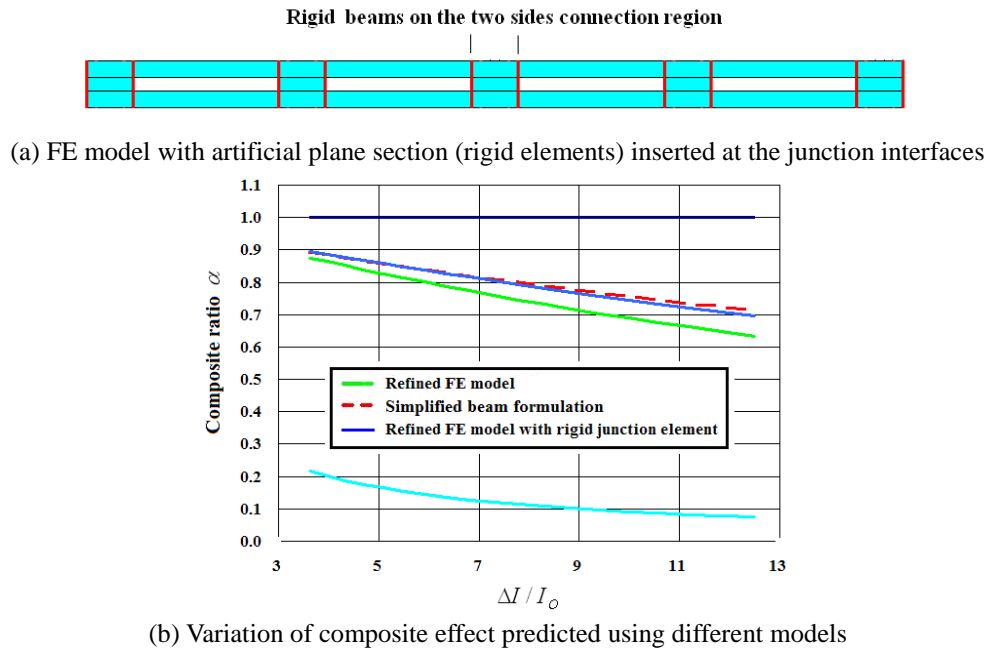
Fig. 8 Evaluation of effect of the plane section assumption on prediction accuracy

(a) Axial stress distribution near the connection region

(b) XY shear stress distribution near the connection region

Fig. 9 Stress concentration around a connection region

The deviation from the plane section assumption may be attributed to the following mechanisms of local deformation around the connection regions:

1) Local deformation within the main beam sections in the vicinity of the shear connectors, i.e., the Saint-Venant's effect, as can be observed from the stress distribution from a FE analysis shown in Fig. 9(a);

2) The deformation within the connectors, as depicted in Fig. 9(b), causing a relative displacement between the top and bottom of a connector, or "shear slide" in a generic sense. The effect due to the shear slide of the connectors could be significant in a CBDSCR with slender connectors (i.e., large g/l ratio) and when the number of connectors is small.

5.2 Modification to the basic beam formulation

To take into account the above mentioned deviations from the idealised beam formulation, a modification is considered herein. If the relative displacement mainly comes from the shear deformation of the connectors, i.e., the "shear slide", a theoretical solution of the additional deflection in the beam due to such an effect has been derived previously for a simply supported composite beam (Nie and Cai 2003), as follows:
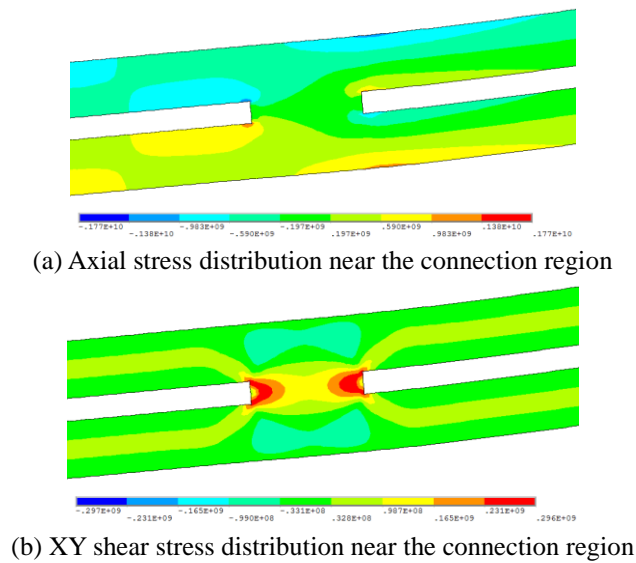
a) Concentrated load at mid span

$$\Delta d \approx \frac{PL^2 A_B A_T d_C}{4hKn[A_B A_T d_c^2 + (A_B + A_T)(I_B + I_T)]}$$ (18a)

b) Uniformly distributed load

$$\Delta d \approx \frac{qL^3 A_B A_T d_c}{8hKn[A_B A_T d_c^2 + (A_B + A_T)(I_B + I_T)]}$$ (18b)

where $d_C = d_T + d_B$, $h = h_T + h_B$. K is the shear stiffness of the connector.

In a CBDSCR, the overall effect of the local deformation causes a further increase of the beam deflection, and hence a further reduction of the beam stiffness. In this respect, Eq. (18) may be adopted in an extended manner, with changes of $d_C = d_T/2 + h_B/2 + g$ and $h = h_T + h_B + g$, whereas the shear stiffness of the connector K is modified to K_{eq}, which denotes an equivalent stiffness of the shear connection region in a CBDSCR and accounts for all local effects around a connector, including the shear slide. The basic shear stiffness of the connection region, as schematically shown in Fig. 10, may be calculated as
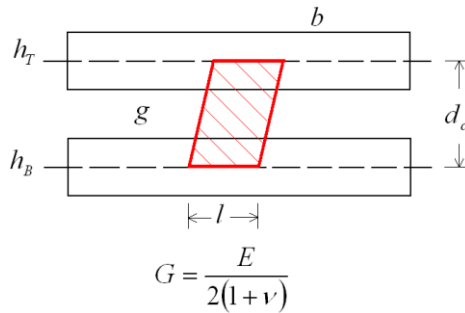
$$K_{shear} = \frac{Ebl}{2(1+v)d_c}$$ (19)

$$G = \frac{E}{2(1+v)}$$

Fig. 10 Calculation of the basic shear stiffness K_{shear}

The equivalent K_{eq} is related to K_{shear} by a reduction factor φ

$$K_{eq} = \varphi K_{shear} \tag{20}$$

The approximation of φ may be obtained by an empirical method. As far as the strain distribution along the section depth is concerned, it can be envisaged that φ is primarily a function of the parameters relating to the local deformations, namely h_T, h_B, g and l, or in a more general sense the normalised parameters of h_B/h_T, g/h_T and l/h_T. Thus

$$\varphi = \varphi\left(\frac{h_B}{h_T}, \frac{g}{h_T}, \frac{l}{h_T}\right) \tag{21}$$

The actual function may be established numerically through finite element calculations. For the FE analysis, the top beam is assumed to have a reference depth of h_T=0.1 m, while all the other dimensions are assigned subsequently in accordance with the specified ratios, and the material is assumed to be the same. h_B/h_T is assumed to vary from 1 to 3, g/h_T from 0.0 to 1.0, l/h_T from 0.2 to 8.0. These ranges are chosen to cover most of practical CBDSCR cases. Totally 75 CBDSCR models are constructed and analysed using FE model to derive the empirical φ. The results are summarised in Table 5.

The modified composite ratio α can be calculated by the following simple steps:

1) Use the composite ratio α in Eq. (17) to calculate the deflection of the CBDSCR without considering the local deformation;

2) Use Eqs. (18), (20), (21) and Table 5 to calculate the additional deflection of a CBDSCR.

3) Use the summation of the two deflections above to calculate the modified composite ratio α.

It should be noted that Table 5 has been generated from FE analysis for coupled beams with the same material, but it is not restricted to single-material coupled beams and is applicable to

Table 5 φ as a function of h_B/h_T, g/h_T and l/h_T

$\frac{h_B}{h_T}=1$		g/h_T					$\frac{h_B}{h_T}=2$		g/h_T				
		0.00	0.25	0.50	0.75	1.00			0.00	0.25	0.50	0.75	1.00
	0.2	5.643	1.520	0.606	0.324	0.208		0.2	4.474	1.678	0.811	0.488	0.344
	0.5	3.321	1.507	0.897	0.591	0.422		0.5	2.463	1.219	0.802	0.577	0.439
$\frac{l}{h_T}$	1.0	1.964	1.053	0.744	0.565	0.452	$\frac{l}{h_T}$	1.0	1.728	0.903	0.653	0.517	0.428
	2.0	1.196	0.661	0.477	0.372	0.306		2.0	1.211	0.650	0.494	0.413	0.360
	4.0	0.879	0.518	0.374	0.288	0.235		4.0	0.845	0.470	0.365	0.313	0.2749
	8.0	0.940	0.767	0.605	0.477	0.388		8.0	0.714	0.504	0.416	0.367	0.335

$\frac{h_B}{h_T}=3$		g/h_T				
		0.00	0.25	0.50	0.75	1.00
	0.2	5.080	2.168	0.598	0.214	0.114
	0.5	2.613	1.357	0.373	0.160	0.090
$\frac{l}{h_T}$	1.0	1.760	0.942	0.230	0.111	0.068
	2.0	1.216	0.665	0.149	0.078	0.051
	4.0	0.795	0.332	0.107	0.060	0.040
	8.0	0.543	0.269	0.112	0.067	0.046

Table 6 Comparison of maximum deflections of 12 CBDSCR beams

Beam	FE model δ_{max} (mm)	Basic beam formulation			With local deformation correction		
		α	δ_{max} (mm)	Error	α	δ_{max} (mm)	Error
1	0.164	0.88	0.159	-3.1%	0.73	0.164	-0.1%
2	0.495	0.90	0.483	-2.5%	0.73	0.495	0.0%
3	0.059	0.64	0.054	-8.3%	-	-	-
4	0.015	0.65	0.013	-7.8%	-	-	-
5	0.152	0.93	0.150	-1.2%	0.73	0.153	0.3%
6	0.149	0.96	0.146	-2.2%	0.73	0.149	0.0%
7	0.148	0.86	0.142	-3.9%	0.60	0.148	0.0%
8	0.123	0.82	0.116	-5.8%	0.48	0.123	-0.1%
9	0.151	0.94	0.148	-2.1%	0.57	0.151	-0.1%
10	0.144	0.98	0.142	-1.4%	0.81	0.144	-0.3%
11	0.088	0.90	0.084	-4.6%	0.72	0.088	-0.2%
12	0.052	0.92	0.049	-5.8%	0.72	0.052	-0.0%

(a) α vs. $\Delta I/I_O$

(b) α vs. n
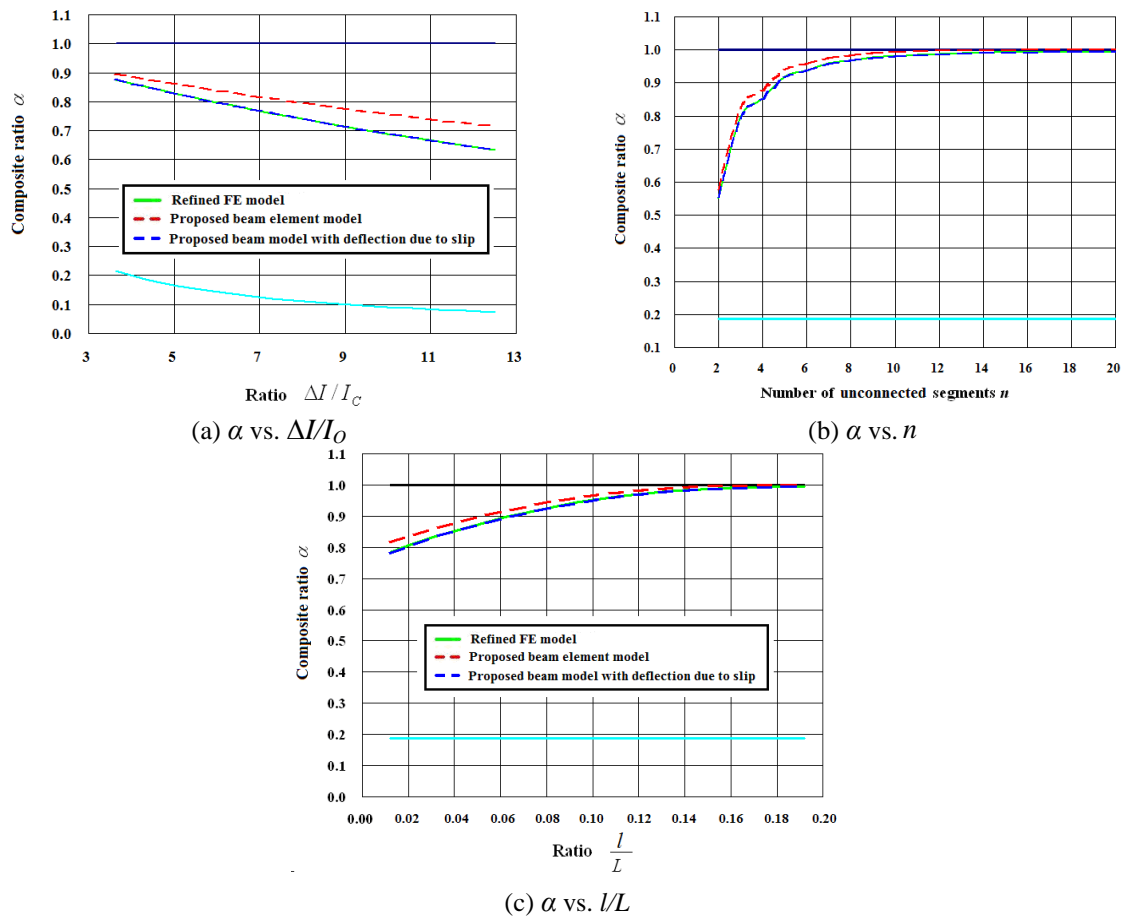
(c) α vs. l/L

Fig. 11 Improvement of the accuracy of the proposed method considering additional deflection due to local deformation

different material cases as far as the effect of local deformation concerned is along the depth of the coupled beam. For beams with wide flanges where local deformation over the width of the flange may become a factor, the exact modification pertaining to the local deformation should be treated accordingly and this is not covered in Table 5.

The modified composite ratio α for the cases described in Section 4.3 is provided in Fig. 11. It can be observed that the results match the FE results closely, as can be expected due to the empirical modification, and comparing with the un-modified results the accuracy is markedly improved. Finally, the 12 CBDSCR beams studied in Section 4.2 (shown in Table 4) are re-calculated and the results are summarised in Table 6. Note that these beam cases are not involved in the generation of the modification factors in Table 5. Again, a marked improvement of the accuracy is achieved. The maximum error which happens in beam-12 is reduced to 0.8% from 5.8% when the local deformation was not considered.

6. Conclusions

This paper presents an analytical approach for the calculation of the composite effect and the bending stiffness of a special class of composite beams, called CBDSCR, where discrete shear connectors are employed as the coupling mechanism. A coupled beam element is established for the unconnected segments in accordance with the compatibility relations at the junctions between an unconnected segment and the connection regions. On this basis, the deflection and the stiffness of the entire beam are constructed, and an analytical solution for CBDSCR with evenly distributed connectors is deduced from assembling the global beam stiffness matrix for a broad range of the CBDSCR configurations.

Comparison of the basic analytical solution with results from refined finite element models shows a reasonably good agreement. Results also show that when a significant connector length, e.g., around or above the total beam depth, is involved, the influence of the connector length can be significant, and the analytical solution with the consideration of the connector length is capable of handling well this factor.

To further improve the accuracy of the analytical solution, a modification factor is introduced to compensate for the local deformations around the junction areas that lead to the relative axial displacements (or in a general sense "shear slips") between the top and bottom beams. The modification factor is related to three dimensionless parameters, and the detailed relationships are established by means of an empirical method using data generated from FE models. With the incorporation of the modification factor the analytical solutions are found to match very well the FEA results.

The proposed general solution of CBDSCR provides a simple and yet sufficiently accurate means for modular building designers to determine desirable coupling configurations and calculate the stiffness and deformations of this type of beams. The basic formulation and the modification scheme are readily applicable to coupled beams with different materials as well as single material. The specific modification factors may also be applied for different material cases as long as the local deformation effect is primarily concerned about the distribution over the depth of the coupled beam. For coupled beams involving wide flanges where the local deformation across the width of the flange may also have an influence on the behaviour of the coupled beam, extended finite element analysis may be required to generate the specific modification data.

Acknowledgements

References

Al-deen, S., Ranzi, G. and Vrcelj, Z. (2011), "Full-scale long-term experiments of simply supported composite beams with solid slabs", *J. Construct. Steel Res.*, **67**(3), 308-321.

Berczyński, S. and Wróblewski, T. (2005), "Vibration of steel–concrete composite beams using the Timoshenko beam model", *J. Vib. Control*, **11**, 829-848.

Gianluca, R. (2008), "Locking problems in the partial interaction analysis of multi-layered composite beams", *Eng. Struct.*, **30**(10), 2900-2911.

Lawson, R.M. (2007), *Building design using modules*, Steel Construction Institute's Publication 348, Ascot, UK.

Liang, Q.Q., Uy, B., Bradford, M.A. and Ronagh, H.R. (2004), "Ultimate strength of continuous composite beams in combined bending and shear", *J. Construct. Steel Res.*, **60**(8), 1109-1128.

Newmark, N.M., Siess C.P. and Viest I.M. (1951), "Tests and analysis of composite beams with incomplete interaction", *Proc. Soc. Exp. Stress Anal.*, **9**(1), 75-92.

Nie, J. and Cai, C.S. (2003), "Steel-concrete composite beams considering shear slip effects", *J. Struct. Eng.*, **129**(4), 495-506.

Nguyen, Q.H., Hjiaj, M. and Aribert, J.M. (2003), "A space-exact beam element for time-dependent analysis of composite members with discrete shear connection", *J. Construct. Steel Res.*, **66**(11), 1330-1338.4.

Nguyen, Q.H., Hjiaj, M., Uy, B. and Guezouli, S. (2009), "Analysis of composite beams in the hogging moment regions using a mixed finite element formulation", *J. Construct. Steel Res.*, **65**(3), 737-748.

Nguyen, Q.H., Hjiaj, M. and Guezouli, S. (2011), "Exact finite element model for shear-deformable two-layer beams with discrete shear connection", *Finite Elem. Anal. Des.*, **47**(7), 718-727.

Razaqpur, A.G. and Nofal, M. (1989), "A finite element for modelling the nonlinear behavior of shear connectors in composite structures", *Comput. Struct.*, **32**(1), 169-174.

Ranzi, G., Gara, F. and Ansourian, P. (2006), "General method of analysis for composite beams with longitudinal and transverse partial interaction", *Comput. Struct.*, **84**(31-32), 2373-2384.

Ranzi, G. and Zona, A. (2007), "A steel-concrete composite beam model with partial interaction including the shear deformability of the steel component", *Eng. Struct.*, **29**(11), 3026-3041.

Ranzi, G., Dall'Asta, A., Ragni, L. and Zona, A. (2010), "A geometric nonlinear model for composite beams with partial interaction", *Eng. Struct.*, **32**(5), 1384-1396.

Salari, M.R., Spacone, E., Shing, P.B. and Frangopol, D.M. (1998), "Nonlinear analysis of composite beams with deformable shear connectors", *J. Struct. Eng.*, **124**(10), 1148-1158.

Wright, H.D. (1990), "The deformation of composite beams with discrete flexible connection", *J. Construct. Steel Res.*, **15**(1-2), 49-64.